



Increased Pressure and Contact Area in Rotator Cuff Crossed versus Simple Transosseous Repair

Mayor presión y área de contacto en reparación transósea cruzada de manguito rotador versus reparación simple

Julio José Contreras¹ Rodrigo Liendo² Francisco Soza²

¹Instituto Traumatológico, Santiago, RM, Chile

²Pontificia Universidad Católica de Chile, Santiago, RM, Chile

Address for correspondence Julio José Contreras Fernández, Instituto Traumatológico, Santiago, RM, Chile
(e-mail: juliocontrerasmd@gmail.com).

Rev Chil Ortop Traumatol 2021;62(3):e159–e167.

Abstract

Objective To compare the pressure and contact area at the tendon-footprint interface of a repair performed with simple and crossed transosseous sutures.

Methods Twelve lamb shoulders were used to simulate a rotator cuff tear. The contact area at the tendon-footprint interface was measured with pressure-sensitive films; then, the pressure was measured with a digital sensor. The baseline pressure was recorded during the application of a cyclic load and at the end of the intervention. A total of 2 repairs were compared: 2 transosseous sutures with single knots (STO; n = 6) and 2 transosseous sutures with crossed knots (TOC; n = 6) using FiberWire #2. In total, 1,400 cycles were performed, with a frequency of 2.5 Hz and a load of 5 N. The Mann-Whitney test was used. Values of $p < 0.05$ were considered significant.

Results The TOS repair presented $50.9 \pm 12.7\%$ of pressure distribution compared to $72.2 \pm 5.3\%$ in the TOC repair ($p < 0.009$). The mean pressure in the TOS repair was of 0.7 ± 0.1 MPa compared to 1.1 ± 0.2 MPa in the TOC repair ($p < 0.007$). The TOS repair registered a basal pressure of 5.3 ± 5.3 N, a final pressure of 3.8 ± 4.6 N, and a variation of $51.7 \pm 38\%$. The TOC repair registered a basal pressure of 10.7 ± 1.8 N, a final pressure of 12.9 ± 8.7 N, and a variation of $114.9 \pm 65.9\%$ ($p < 0.044$; $p < 0.022$; and $p < 0.017$ respectively).

Conclusion The TOC repair presents higher pressure at the tendon-bone interface, less loss of contact force under cyclic loads, and a better distribution of force on the footprint when compared with the TOS repair, which could translate into better tendon healing.

Level of Evidence Basic Science Study.

Keywords

- ▶ rotator cuff
- ▶ pressure
- ▶ suture
- ▶ suture techniques
- ▶ tendon injuries
- ▶ tendons

received
June 28, 2020
accepted
August 6, 2021

DOI <https://doi.org/10.1055/s-0041-1740546>.
ISSN 0716-4548.

© 2021. Sociedad Chilena de Ortopedia y Traumatología. All rights reserved.

This is an open access article published by Thieme under the terms of the Creative Commons Attribution-NonDerivative-NonCommercial-License, permitting copying and reproduction so long as the original work is given appropriate credit. Contents may not be used for commercial purposes, or adapted, remixed, transformed or built upon. (<https://creativecommons.org/licenses/by-nc-nd/4.0/>)

Thieme Revinter Publicações Ltda., Rua do Matoso 170, Rio de Janeiro, RJ, CEP 20270-135, Brazil

Resumen

Objetivo Comparar la presión y el área de contacto en la interfase tendón-huella de una reparación realizada con suturas transóseas simples y cruzadas.

Métodos Se utilizaron doce hombros de cordero para simular una rotura de manguito rotador. Se midió el área de contacto en la interfase tendón-huella con láminas sensibles a presión; luego, se midió la presión con un sensor digital. Se registró la presión basal durante la aplicación de carga cíclica y al final de la intervención. Se compararon 2 reparaciones: 2 túneles transóseos con nudos simples (TOS; $n = 6$) y 2 túneles transóseos con nudos cruzados (TOC; $n = 6$), utilizando FiberWire #2. Se realizaron 1.400 ciclos, con una frecuencia 2,5 Hz y una carga de 5 N. Se utilizó la prueba de Mann-Whitney, y se consideraron significativos valores de $p < 0,05$.

Resultados La reparación TOS presentó un $50,9 \pm 12,7\%$ de distribución de presiones en comparación con $72,2 \pm 5,3\%$ en la reparación TOC ($p < 0,009$). La presión promedio en la reparación TOS fue $0,7 \pm 0,1$ MPa en comparación con $1,1 \pm 0,2$ MPa en la reparación TOC ($p < 0,007$). La reparación TOS registró una presión basal de $5,3 \pm 5,3$ N, presión final de $3,8 \pm 4,6$ N, y una variación de $51,7 \pm 38\%$. La reparación TOC registró una presión basal de $10,7 \pm 1,8$ N, presión final de $12,9 \pm 8,7$ N, y una variación de $114,9 \pm 65,9\%$ ($p < 0,044$; $p < 0,022$; y $p < 0,017$, respectivamente).

Conclusión La reparación TOC presenta mayor presión a nivel de la interfase tendón-hueso, menor pérdida de fuerza de contacto ante cargas cíclicas, y una mejor distribución de fuerza en la huella al comparar con la reparación TOS, lo que se podría traducir en mejor cicatrización tendínea.

Nivel de Evidencia Estudio de ciencia básica.

Palabras Clave

- ▶ manguito de los rotadores
- ▶ presión
- ▶ sutura
- ▶ técnicas de sutura
- ▶ traumatismos de los tendones
- ▶ tendones

Introduction

The performance of arthroscopic rotator cuff repairs has been increasing constantly in recent times.¹ Short and long-term clinical and functional results are good to excellent in most cases;²⁻⁵ however, rerupture rates are still considerable, ranging from 11% to 68% in selected series, even reaching 94% in some studies.⁶⁻⁸

The surgery for rotator cuff repair seeks to establish a fibrovascular interface between the tendon and the footprint, which is required for the healing and restoration of the fibrocartilaginous insertion (entheses); to do so, the construct must maximize the pressurized contact between tendon and bone while maintaining the mechanical resistance against a physiological load.^{9,10}

Several anatomical factors favor healing, including a good construct tension, proper tissue perfusion, reduced micromotion at the tendon-footprint interface, and adequate footprint pressure and contact area.¹¹ The underlying principle is that a greater tendon-to-bone contact area, both in terms of magnitude and distribution, will increase tendon healing.¹²

The double row (DR) repair increases resistance to load-related failure, improves contact areas and pressures, and decreases gap formation at the tendon-footprint interface compared to the single row (SR) repair.^{5,13} However, anchors provide low resistance, in addition to being prone to loosen in osteoporotic bone; as such, they result in poor contact at the level of the supraspinatus tendon footprint, and may

cause greater tuberosity osteolysis, making revision a challenge and increasing costs.¹⁴⁻¹⁸

The transosseous (TO) technique enables the maximization of the contact area at the tendon-footprint interface¹⁹ and reduce movement at the tendon-bone interface.²⁰ In addition to this mechanical aspect, the TO technique enables the accurate preparation of bone side of the lesion without risks or complications, including anchor removal and/or greater tuberosity osteolysis.^{21,22}

Transosseous suture techniques are efficient and reproducible for the arthroscopic repair of rotator cuff tears.²³ Moreover, there is a greater potential for healing due to direct contact between tendon and bone (without intervening anchor material) and mesenchymal stem cells from the bone tunnels at the proximal humerus.²⁴⁻²⁷

Due to these advantages, our team designed a device capable of performing oblique TO tunnels, enabling repairs with simple or crossed sutures.

The present study aims to compare the pressure and contact area at the tendon-footprint interface in repairs performed with simple or crossed TO sutures. Our hypothesis is that the crossed configuration will result in a larger contact area and a lower pressure drop after cyclic loading.

Materials and Methods

Animal Model

A total of 12 fresh frozen shoulders from 6-month-old lambs (*Ovis orientalis aries*) were obtained from a local company

(oyster cut, Frigorífico Simunovic Ltda., Punta Arenas, Región de Magallanes y Antártica Chilena, Chile). They were thawed at room temperature the night before the biomechanical tests. The infraspinatus tendon was selected because its anatomical and functional features are equivalent to those of the human supraspinatus tendon.²⁸ The specimens were dissected in a standardized way, removing all the soft tissue adjacent to the humeral shaft, and the subscapular and the supraspinatus fossae of the scapula to isolate the infraspinatus muscle and its tendon. No specimen had any rotator cuff abnormalities. Next, a scapular osteotomy was performed at the level of the spine, sparing the infraspinatus muscle attachment, to enable muscle manipulation without tearing it apart (► **Figure 1**). Lastly, 2 perforations were made 1 cm from the medial edge of the scapula, separated by 1 cm on each side of the scapular spine, with a 5.0-mm drill bit, to enable the osteotomized fragment to be hooked to the load cell (► **Figures 2 and 3**). Specimens were irrigated intermittently with 0.9% NaCl solution throughout each test to prevent sample dehydration.

A tailored system generated cyclic tensions at the level of the infraspinatus muscle and tendon (► **Figure 4**). The model had three fundamental parts: a modular support with adjustable height, an adjustable support for guidance of the suture system, and a load cell digitally regulated using the Arduino (open source) software.

The humeral shaft was fixated in a polyvinyl chloride (PVC) plastic cylinder with plaster. Then, the modular support was adjusted to ensure the tendon was parallel to the



Fig. 1 Anatomical dissection of the infraspinatus tendon of a lamb specimen. Standardized anatomical dissection, removing all the soft tissue adjacent to the humeral shaft and the subscapular and supraspinatus fossae of the scapula to isolate the infraspinatus muscle and its tendon. An arrow indicates the infraspinatus tendon, the delta (δ) shows the infraspinatus muscle, and the asterisk marks the scapular osteotomy at level of the spine, sparing the infraspinatus muscle attachment.

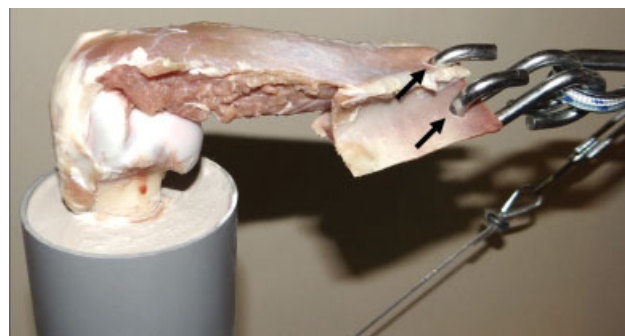


Fig. 2 Scapular foramina for the fixation of the infraspinatus muscle (anterior view). Two perforations were made 1 cm from the medial edge of the scapula, separated by 1 cm on each side of the scapular spine, with a 5.0-mm drill bit, to hook the osteotomized fragment to the load cell (anterior view).

horizon (using a level), achieving a traction angle of 0° in abduction.

Rotator Cuff Tear

In each humeral head, the orientation of the greater tuberosity was identified and demarcated with a 1.5-mm Kirschner needle. Next, the tip of the tuberosity was identified and, 10 mm laterally to it, a full thickness, 20-mm wide tear was

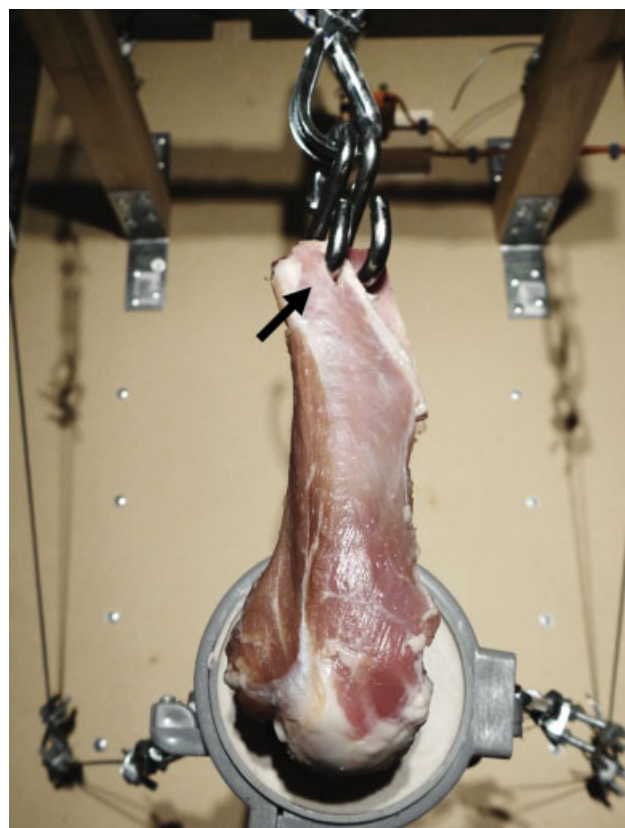


Fig. 3 Scapular foramina for the fixation of the infraspinatus muscle (superior view). Two perforations were made 1 cm from the medial edge of the scapula, separated by 1 cm on each side of the scapular spine, with a 5.0-mm drill bit, to hook the osteotomized fragment to the load cell (superior view). The arrow shows how the muscle remains undamaged, with no tears.

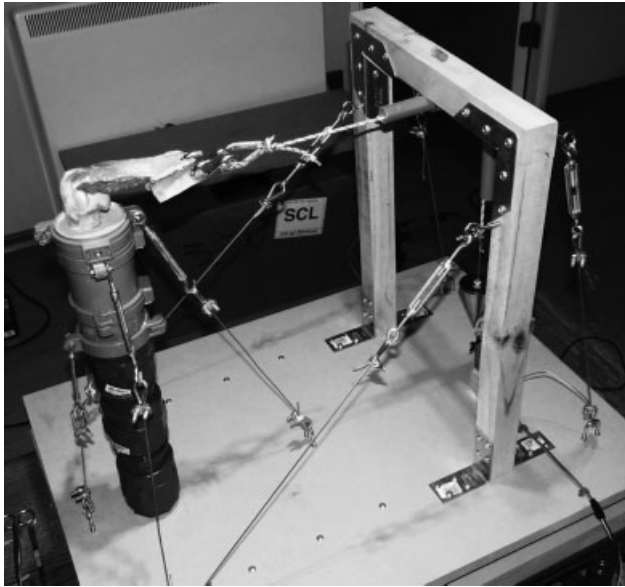


Fig. 4 Cyclic stress model. The model consisted of a height-adjustable modular support, an adjustable support for the guidance of the suture system, and a load cell. The humeral shaft was fixated in a PVC plastic cylinder with plaster.

made with a #15 scalpel, releasing the entire tendon attachment from the footprint, and then flattening it with a rasp to facilitate the placement of pressure sensors (→ **Figure 5**).

Measurement of Pressure and Contact Area at the Tendon-Footprint Interface

The contact area was measured at the beginning of the repair, while pressure was determined at the beginning, during and at the end of cyclic loading.

First, at time zero, the contact area at the tendon-footprint interface was measured (percentage and mean pressure [MPa]) using a set of colorimetric, pressure-sensitive films (Prescale Ultra Low Pressure Fuji Photo Film, C. Itoh & Co, New York, NY, US) covered with a plastic sheet to protect them from tissue moisture. These films were positioned on the previously-flattened surface of the footprint. Subsequently, the repair was carried out. The films were then digitized and analyzed with a previously-calibrated scanner and software (Fujifilm Analysis System for Prescale, Tekscan, Inc., South Boston, MA, US).

A digital pressure sensor (Flexiforce Sensor, Tekscan) was used to measure the pressure at the tendon-footprint interface. The sensor was positioned between the tendon and the footprint, and remained fixed by the repair; it records pressure changes over time and stores them in a computer for later analysis (N). The baseline pressure was recorded at the beginning of the experiment (time zero), during cyclic loading, and at the end of the intervention.

Repair of Rotator Cuff Tear with Transosseous Sutures and Biomechanical Testing

The repairs were performed with a #2 polyester braided, non-absorbable polymer suture with a long-chain polyeth-

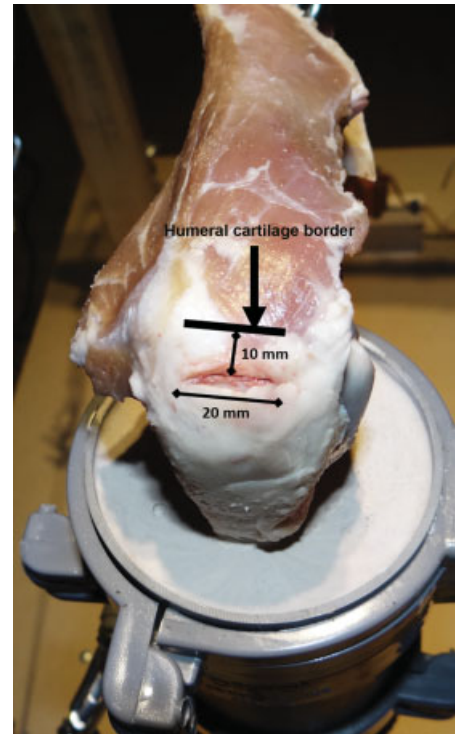


Fig. 5 Rotator cuff tear. The arrow marks the edge of the humeral cartilage, which was palpated and marked with a needle. Next, 10 mm lateral to it, a full thickness, 20-mm wide tear was made.

ylene core (FiberWire; Arthrex, Naples, FL, US), the most commonly-used size in arthroscopic shoulder surgery.

The TO tunnels were prepared with a device previously designed by our team and used in previous models to generate oblique tunnels (→ **Figure 6**).

Two different TO repairs were performed, always by the same surgeon (JC) to reduce interoperator variability: 1) two TO tunnels with single knots (TOS) (→ **Figure 7A**) on six lamb shoulders; and 2) two TO tunnels with crossed knots (TOC) (→ **Figure 7B**). Both repairs were made with #2 FiberWire suture, using either the “Tennessee slider” knot for the TOS repair or the “Revo-SCOI” knot for the TOC repair. No tensiometer was used for knotting.

The repair was pretensioned with 10 N for 2 minutes. The load cell was then programmed to 1,400 cycles, with a frequency of 2.5 Hz and a load of 5 N. These parameters were defined based on those used in similar studies,^{29,30} and they reflect the initial postoperative rehabilitation period (two weeks) with passive exercises and pendular movements.

Statistical Analysis

The results were presented as means and standard deviations. Given the small sample with non-normal distribution (as demonstrated by the Shapiro-Wilk test), the statistical test for the non-parametric variables (that is, the Mann-Whitney test) was used. All data were analyzed using the STATA (StataCorp LLC, College Station, TX, US) software, version 14. Significance was set at $p < 0.05$.

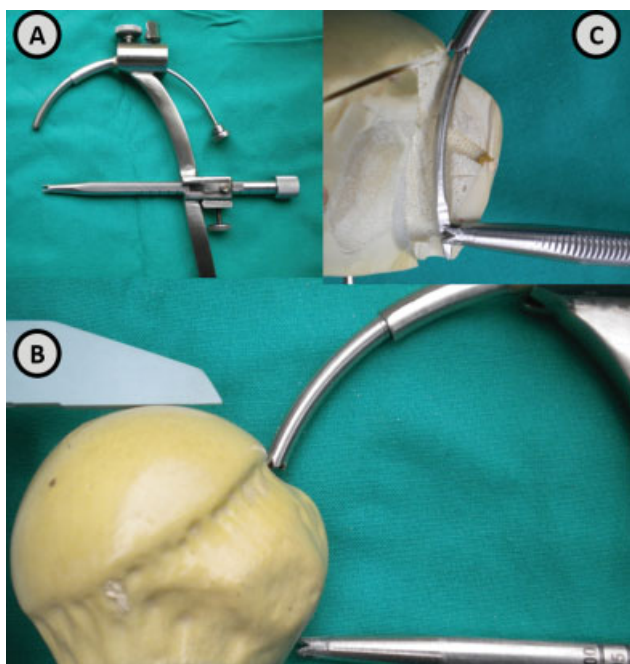


Fig. 6 Device for making transosseous oblique tunnels. Inset A shows the transosseous suture device used. Inset B shows the proper positioning of the device in relation to the greater tuberosity. Inset C shows a section of an artificial bone model and the trajectory of the oblique tunnel.

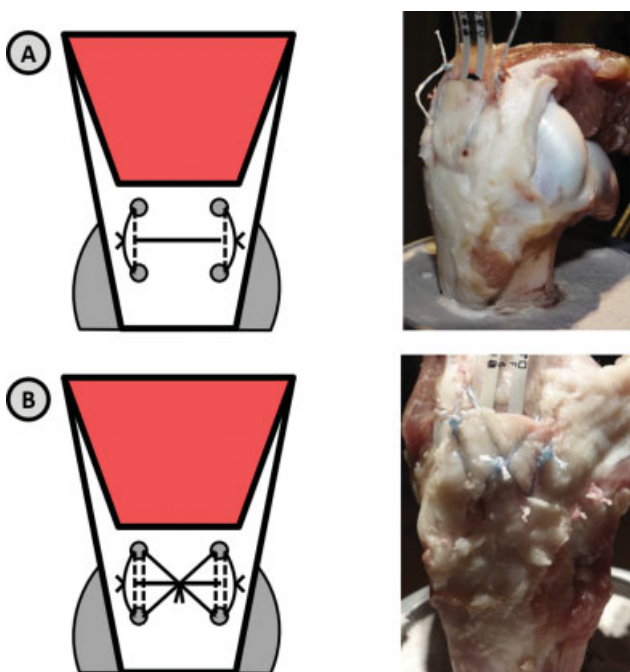


Fig. 7 Repair with transosseous sutures. Inset A shows the transosseous repair with single knots, and inset B shows the repair with crossed knots.

Results

The contact area at the tendon-footprint interface at time zero was 1.4-fold greater in the TOC repair. Pressure distri-

bution was of $50.9 \pm 12.7\%$ for the TOS, and of $72.2 \pm 5.3\%$ for the TOC repair ($p < 0.009$) (**Figure 8**).

Pressure at the tendon-footprint interface at time zero (measured with a pressure-sensitive sheet) was 1.6-fold greater in the TOC repair. The mean pressure was of 0.68 ± 0.13 MPa in the TOS, and of 1.1 ± 0.2 MPa in the TOC repair ($p < 0.007$) (**Figure 8**).

Regarding pressure at the tendon-footprint interface in response to cyclic loading (measured with a digital pressure sensor), both repair models presented a self-reinforcing mechanism during increased cyclic stress (**Figure 9**).

For the TOS repair, the pressure was of 5.3 ± 5.3 N at baseline, and of 3.8 ± 4.6 N at the end of the intervention, with a $51.7 \pm 38.0\%$ variation after 1,400 tension cycles. For the TOC repair, the pressure was of 10.7 ± 1.8 N at baseline, and of 12.9 ± 8.7 N at the end of intervention, with a $114.9 \pm 65.9\%$ variation ($p < 0.044$; $p < 0.022$; and $p < 0.017$ respectively) (**Table 1**).

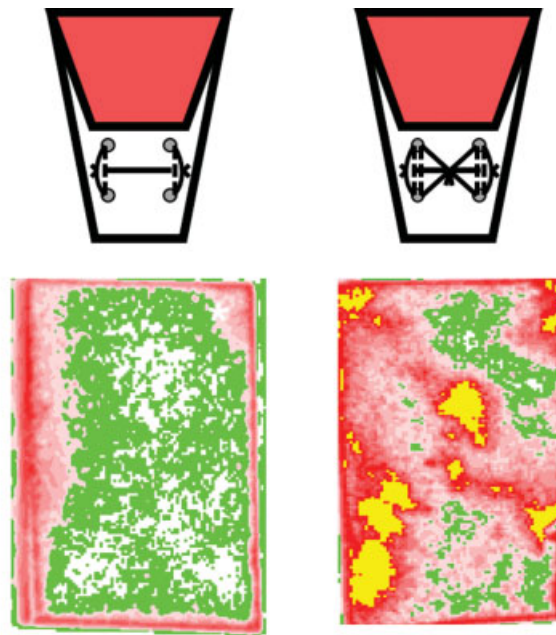
Discussion

The main finding of the present study was that the TOC repair results in greater pressure at the level of the tendon-bone interface at time zero, lower loss of contact force due to cyclic loading over time, and a better distribution of force at the footprint when compared to the TOS repair.

This is an important finding because, when using arthroscopic instruments to perform TO sutures, the TOC technique would improve pressure and the distribution of force by only modifying a surgical gesture. The present is the first report of such biomechanical advantage.

These findings were expected, since the TOC repair distributes the pressure in an area that had not been previously loaded; this is directly related to the self-reinforcement mechanism described by Burkhart et al.²⁷ in 2009, in which an increased stress applied to the construct amplifies resistance to structural failure by progressively increasing compression forces at the tendon footprint. The compressive forces created at the footprint increase the frictional resistance between tendon and bone, thus reducing the formation of gaps between them.²⁷ Wedging of the angle between the suture material and the bone is formed as the tendon is progressively stressed; in addition, at the coronal plane, suture geometry changes from rectangular to trapezoidal as the tensile load increases.²⁷ This results in an elastic deformation of the tendon, creating a compression force perpendicular to the bone surface, which increases according to the tensile load²⁷ (**Figure 10**).

The high standard deviation values for baseline and final pressure levels both in the TOS and TOC repair is probably associated with knot tension because, in the TOC repair, the pressure at the footprint level is directly related to the tension delivered by the knot, which was not quantitatively measured. Although all procedures were performed by the same surgeon, there is a risk of internal variability. Clinically, the tension delivered in the anchor repair with and without knots is a constant challenge in arthroscopic rotator cuff repair surgery. The intraoperative use of blood pressure monitors could improve the reproducibility of these techniques.



Parameter	Single-knot transosseous suture	Crossed-knot transosseous suture	p-value
Pressure distribution area	50.94% ± 12.69%	72.24% ± 5.32%	$p < 0.009$
Mean pressure	0.68 ± 0.1 Pa	1.07 ± 0.1 Pa	$p < 0.007$
Maximum pressure	2.74 ± 0.45 Pa	3.06 ± 0.00 Pa	NS

Fig. 8 Contact area and pressure at the tendon-footprint interface at time zero. The contact area was measured with Fujifilm. The areas in red represent a higher contact pressure and those in green represent a lower contact pressure. The table shows quantitative results expressed as means and standard deviations. Abbreviation: NS, not significant.

Our findings are comparable to those of biomechanical studies^{5,13} with DR repairs which have shown an increase in resistance to load-induced failure, improved contact areas and pressure, and a decrease in gap formation at the tendon-footprint interface compared to SR repairs.^{5,13}

Ng et al.³¹ used infraspinatus tendons from a porcine model to compare the pressure distribution in three DR configurations (suture bridge; two medial and one lateral

anchors; and one medial and two lateral anchors). These authors showed that this technique not only results in a good footprint contact area (75%, 75%, and 73% respectively), but that the use of a 3- or 4-anchor configuration produces a similar footprint contact area in medium tears (no greater than 1.5 cm × 2.5 cm). These findings are consistent with those of the present study, demonstrating at least one equivalence between the TOC repair and the suture bridge

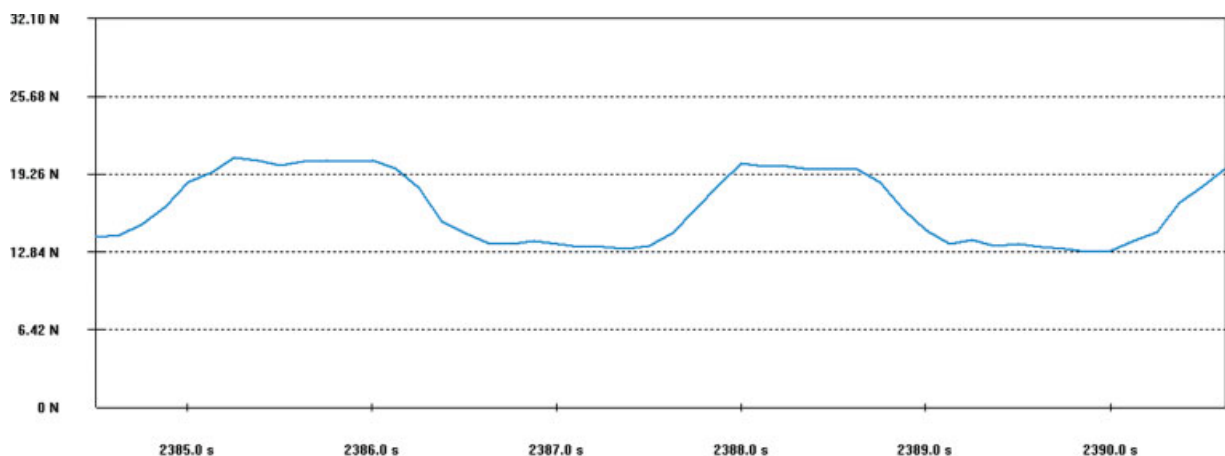


Fig. 9 Example of pressure measurement under cyclic loading, demonstrating the self-reinforcement mechanism in transosseous repair.

Table 1 Pressure during cyclic loads

Parameter (N)	Repair type			
	Simple transosseous repair		Crossed transosseous repair	
	Mean	SD	Mean	SD
Baseline pressure	5.30	5.30	10.71	1.78
Pressure at 25%	4.91	5.59	10.88	4.95
Peak at 25%	7.45	7.68	16.36	6.48
Pressure at 50%	5.18	5.63	13.12	8.09
Peak at 50%	7.34	6.96	17.71	7.36
Pressure at 75%	4.63	5.01	11.98	6.19
Peak at 75%	7.25	6.54	16.52	5.80
Final pressure	3.84	4.56	12.90	8.73
Final peak	6.42	6.34	17.57	8.69
Δ pressure	-1.46	1.85	2.19	7.49
Variation	51.71%	38.00%	114.85%	65.94%

Abbreviations: Δ , force variation; N, newton; SD, standard deviation.

Note: The percentages express cyclic load timing during measurement (25%: 350 cycles; 50%: 700 cycles; 75%: 1,050 cycles; final: 1,400 cycles).

at time zero regarding the pressure distribution area at the tendon-bone interface. Apparently, this equivalence would only occur in this configuration, since Caldow et al.⁹ demonstrated the biomechanical inferiority of the TOS repair regarding contact area, contact pressure, tensile strength, and stiffness compared to the Mason-Allen and DR techniques.

Hinse et al.³² compared the TO technique with sutures, TO with braided tape, and a TO-equivalent (TOE) technique. Although the load at failure was not different between the braided-tape TO and the TOE, the TO with sutures presented significantly less resistance compared to the TOE, indicating

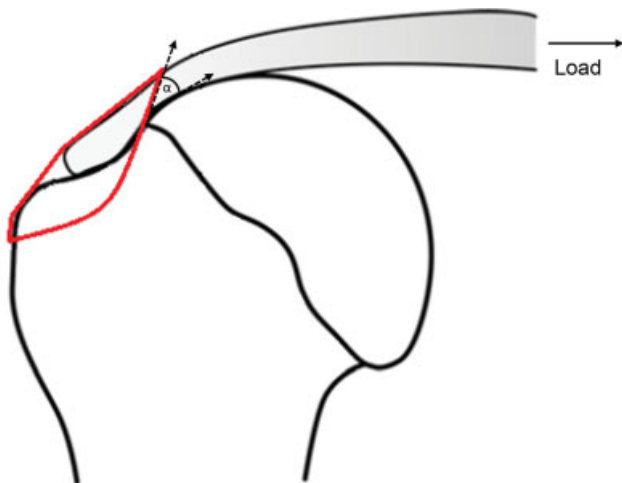


Fig. 10 Schematic drawing of self-reinforcement in transosseous repair showing wedging of the angle between the suture material and the bone as the tendon is progressively stressed, and a change from rectangular to trapezoidal suture geometry in the coronal plane as the tensile load increases.

that the type of material could be an important factor to consider. In addition, even though significant differences were not detected, there was a trend towards a greater loss of footprint coverage with pure TO techniques.

Park et al.¹² compared simple TO suture, SR suture, and SR with mattress suture. They demonstrated that the TO tunnel rotator cuff repair technique generated significantly greater contact and a greater overall pressure distribution over the defined footprint compared to the remaining techniques. However, they did not compare TO with TOE, which are the most relevant techniques today. Tuoheti et al.³³ compared simple TO, and SR and DR sutures, and found out that DR was superior to TO; however, it was a simple TO technique and a DR with mattress sutures, the same weaknesses observed in Park et al.¹² study.

However, these studies only evaluate biomechanical properties regarding pressure magnitude and distribution in addition to load to failure. Apparently, the TO technique would have healing benefits in terms of the supply of the mesenchymal cells, and better tendon vascularization.²⁴⁻²⁶ Using ultrasound, Urita et al.³⁴ demonstrated that vascularization is superior in patients submitted to the TO arthroscopic repair compared to the TOE repair.

A limitation of the present study is the evaluation of biomechanical aspects in an animal model alone; therefore, the findings may be different in human beings and under biological conditions (considering mesenchymal cells and irrigation). The use of human cadaveric shoulders would have been better to represent these biomechanical features. On the other hand, this model standardizes our results, because each sample is six months old, which improves comparability. This is also true for bone mineral density, which was not calculated for our samples, but would have been very similar since the specimens had the same age.

Another important aspect to consider is the clinical relevance of our findings; even though we have demonstrated significant differences in biomechanical factors, many factors play a role in rotator cuff healing, so the clinical impact is unknown.

Conclusion

The TOC repair results in greater pressure at the tendon-bone interface, lower loss of contact force under cyclic loading, and better force distribution at the footprint when compared to the TOS repair.

Acknowledgments

To our family, for their constant support to our research work.

References

- Jancuska J, Matthews J, Miller T, Kluczynski MA, Bisson LJ. A Systematic Summary of Systematic Reviews on the Topic of the Rotator Cuff. *Orthop J Sports Med* 2018;6(09):2325967118797891. Doi: 10.1177/2325967118797891
- Collin P, Colmar M, Thomazeau H, et al. Clinical and MRI Outcomes 10 Years After Repair of Massive Posterosuperior Rotator Cuff Tears. *J Bone Joint Surg Am* 2018;100(21):1854–1863. Doi: 10.2106/JBJS.17.01190
- Collin P, Thomazeau H, Walch G, et al. Clinical and structural outcome twenty years after repair of isolated supraspinatus tendon tears. *J Shoulder Elbow Surg* 2019;28(01):196–202. Doi: 10.1016/j.jse.2018.07.023
- Piper CC, Hughes AJ, Ma Y, Wang H, Neviasser AS. Operative versus nonoperative treatment for the management of full-thickness rotator cuff tears: a systematic review and meta-analysis. *J Shoulder Elbow Surg* 2018;27(03):572–576. Doi: 10.1016/j.jse.2017.09.032
- Rossi LA, Rodeo SA, Chahla J, Ranalletta M. Current Concepts in Rotator Cuff Repair Techniques: Biomechanical, Functional, and Structural Outcomes. *Orthop J Sports Med* 2019;7(09):2325967119868674. Doi: 10.1177/2325967119868674
- Chona DV, Lakomkin N, Lott A, et al. The timing of retears after arthroscopic rotator cuff repair. *J Shoulder Elbow Surg* 2017;26(11):2054–2059. Doi: 10.1016/j.jse.2017.07.015
- Haque A, Pal Singh H. Does structural integrity following rotator cuff repair affect functional outcomes and pain scores? A meta-analysis. *Shoulder Elbow* 2018;10(03):163–169. Doi: 10.1177/1758573217731548
- Galatz LM, Ball CM, Teefey SA, Middleton WD, Yamaguchi K. The outcome and repair integrity of completely arthroscopically repaired large and massive rotator cuff tears. *J Bone Joint Surg Am* 2004;86(02):219–224. Doi: 10.2106/00004623-200402000-00002
- Caldow J, Richardson M, Balakrishnan S, Sobol T, Lee PV, Ackland DC. A cruciate suture technique for rotator cuff repair. *Knee Surg Sports Traumatol Arthrosc* 2015;23(02):619–626. Doi: 10.1007/s00167-014-3474-7
- Desmoineaux P. Failed rotator cuff repair. *Orthop Traumatol Surg Res* 2019;105(1S):S63–S73. Doi: 10.1016/j.otsr.2018.06.012
- Cicak N, Klobucar H, Bicanic G, Trsek D. Arthroscopic transosseous suture anchor technique for rotator cuff repairs. *Arthroscopy* 2006;22(05):565.e1–565.e6. Doi: 10.1016/j.arthro.2005.07.029
- Park MC, Cadet ER, Levine WN, Bigliani LU, Ahmad CS. Tendon-to-bone pressure distributions at a repaired rotator cuff footprint using transosseous suture and suture anchor fixation techniques. *Am J Sports Med* 2005;33(08):1154–1159. Doi: 10.1177/0363546504273053
- Hohmann E, König A, Kat CJ, Glatt V, Tetsworth K, Keough N. Single- versus double-row repair for full-thickness rotator cuff tears using suture anchors. A systematic review and meta-analysis of basic biomechanical studies. *Eur J Orthop Surg Traumatol* 2018;28(05):859–868. Doi: 10.1007/s00590-017-2114-6
- Apreleva M, Ozbaydar M, Fitzgibbons PG, Warner JJ. Rotator cuff tears: the effect of the reconstruction method on three-dimensional repair site area. *Arthroscopy* 2002;18(05):519–526. Doi: 10.1053/jars.2002.32930
- Ma R, Chow R, Choi L, Diduch D. Arthroscopic rotator cuff repair: suture anchor properties, modes of failure and technical considerations. *Expert Rev Med Devices* 2011;8(03):377–387. Doi: 10.1586/erd.11.4
- Kowalsky MS, Dellenbaugh SG, Erlichman DB, Gardner TR, Levine WN, Ahmad CS. Evaluation of suture abrasion against rotator cuff tendon and proximal humerus bone. *Arthroscopy* 2008;24(03):329–334. Doi: 10.1016/j.arthro.2007.09.011
- Ntalos D, Huber G, Sellenschloh K, et al. All-suture anchor pullout results in decreased bone damage and depends on cortical thickness. *Knee Surg Sports Traumatol Arthrosc* 2020;•••. Doi: 10.1007/s00167-020-06004-6
- Godry H, Jettkant B, Seybold D, Venjakob AJ, Bockmann B. Pullout strength and failure mode of industrially manufactured and self-made all-suture anchors: a biomechanical analysis. *J Shoulder Elbow Surg* 2020;29(07):1479–1483
- Imam MA, Abdelkafy A. Outcomes following arthroscopic transosseous equivalent suture bridge double row rotator cuff repair: a prospective study and short-term results. *SICOT J* 2016;2:7. Doi: 10.1051/sicotj/2015041
- Flanagin BA, Garofalo R, Lo EY, et al. Midterm clinical outcomes following arthroscopic transosseous rotator cuff repair. *Int J Shoulder Surg* 2016;10(01):3–9. Doi: 10.4103/0973-6042.174511
- Garofalo R, Castagna A, Borroni M, Krishnan SG. Arthroscopic transosseous (anchorless) rotator cuff repair. *Knee Surg Sports Traumatol Arthrosc* 2012;20(06):1031–1035. Doi: 10.1007/s00167-011-1725-4
- Benson EC, MacDermid JC, Drosdowech DS, Athwal GS. The incidence of early metallic suture anchor pullout after arthroscopic rotator cuff repair. *Arthroscopy* 2010;26(03):310–315. Doi: 10.1016/j.arthro.2009.08.015
- Chillemi C, Mantovani M. Arthroscopic trans-osseous rotator cuff repair. *Muscles Ligaments Tendons J* 2017;7(01):19–25. Doi: 10.11138/mltj/2017.7.1.019
- Tauber M, Koller H, Resch H. Transosseous arthroscopic repair of partial articular-surface supraspinatus tendon tears. *Knee Surg Sports Traumatol Arthrosc* 2008;16(06):608–613. Doi: 10.1007/s00167-008-0532-z
- Campbell TM, Lapner P, Dilworth FJ, et al. Tendon contains more stem cells than bone at the rotator cuff repair site. *J Shoulder Elbow Surg* 2019;28(09):1779–1787. Doi: 10.1016/j.jse.2019.02.008
- Kida Y, Morihara T, Matsuda K, et al. Bone marrow-derived cells from the footprint infiltrate into the repaired rotator cuff. *J Shoulder Elbow Surg* 2013;22(02):197–205. Doi: 10.1016/j.jse.2012.02.007
- Burkhart SS, Adams CR, Burkhart SS, Schoolfield JD. A biomechanical comparison of 2 techniques of footprint reconstruction for rotator cuff repair: the SwivelLock-FiberChain construct versus standard double-row repair. *Arthroscopy* 2009;25(03):274–281. Doi: 10.1016/j.arthro.2008.09.024
- Andres BM, Lam PH, Murrell GA. Tension, abduction, and surgical technique affect footprint compression after rotator cuff repair in an ovine model. *J Shoulder Elbow Surg* 2010;19(07):1018–1027. Doi: 10.1016/j.jse.2010.04.005
- Mahar AT, Moezzi DM, Serra-Hsu F, Pedowitz RA. Comparison and performance characteristics of 3 different knots when tied with 2 suture materials used for shoulder arthroscopy. *Arthroscopy* 2006;22(06):614.e1–614.e2. Doi: 10.1016/j.arthro.2006.02.005

- 30 Wüst DM, Meyer DC, Favre P, Gerber C. Mechanical and handling properties of braided polyblend polyethylene sutures in comparison to braided polyester and monofilament polydioxanone sutures. *Arthroscopy* 2006;22(11):1146–1153. Doi: 10.1016/j.arthro.2006.06.013
- 31 Ng SHA, Tan CHJ. Double-row repair of rotator cuff tears: Comparing tendon contact area between techniques. *World J Orthop* 2020;11(01):10–17. Doi: 10.5312/wjo.v11.i1.10
- 32 Hinse S, Ménard J, Rouleau DM, Canet F, Beauchamp M. Biomechanical study comparing 3 fixation methods for rotator cuff massive tear: Transosseous No. 2 suture, transosseous braided tape, and double-row. *J Orthop Sci* 2016;21(06):732–738. Doi: 10.1016/j.jos.2016.07.001
- 33 Tuoheti Y, Itoi E, Yamamoto N, et al. Contact area, contact pressure, and pressure patterns of the tendon-bone interface after rotator cuff repair. *Am J Sports Med* 2005;33(12):1869–1874. Doi: 10.1177/0363546505278256
- 34 Urita A, Funakoshi T, Horie T, Nishida M, Iwasaki N. Difference in vascular patterns between transosseous-equivalent and transosseous rotator cuff repair. *J Shoulder Elbow Surg* 2017;26(01):149–156. Doi: 10.1016/j.jse.2016.06.010